Altered Heart Rate and Sinoatrial Node Function in Mice Lacking the cAMP Regulator Phosphoinositide 3-Kinase-γ

Robert A. Rose, M. Golam Kabir, Peter H. Backx

Abstract*—**Ablation of the enzyme phosphoinositide 3-kinase (PI3K)γ (PI3K$\gamma^{-/-}$) in mice increases cardiac contractility by elevating intracellular cAMP and enhancing sarcoplasmic reticulum Ca^{2+} handling. Because cAMP is a critical determinant of heart rate, we investigated whether heart rate is altered in mice lacking PI3Kγ. Heart rate was similar in anesthetized PI3K$\gamma^{-/-}$ and wild-type (PI3K$\gamma^{+/+}$) mice. However, IP injection of atropine (1 mg/kg), propranolol (1 mg/kg), or both drugs in combination unmasked elevated heart rates in PI3K$\gamma^{-/-}$ mice, suggesting altered sinoatrial node (SAN) function. Indeed, spontaneous action potential frequency was ≈35% greater in SAN myocytes isolated from PI3K$\gamma^{-/-}$ mice compared with PI3K$\gamma^{+/+}$ mice. These differences in action potential frequency were abolished by intracellular dialysis with the cAMP/protein kinase A antagonist Rp-cAMP but were unaffected by treatment with ryanodine to inhibit sarcoplasmic reticulum Ca^{2+} release. Voltage-clamp experiments demonstrated that elevated action potential frequencies in PI3K$\gamma^{-/-}$ SAN myocytes were more strongly associated with cAMP-dependent increases in L-type Ca^{2+} current ($I_{Ca,L}$) than elevated hyperpolarization-activated current (I_f). In contrast, $I_{Ca,L}$ was not increased in working atrial myocytes, suggesting distinct subcellular regulation of L-type Ca^{2+} channels by PI3Kγ in the SAN compared with the working myocardium. In summary, PI3Kγ regulates heart rate by the cAMP-dependent modulation of SAN function. The effects of PI3Kγ ablation in the SAN are unique from those in the working myocardium. (Circ Res*. 2007;101:1274-1282.**)

Key Words: ion channels ■ electrophysiology ■ action potentials ■ arrhythmia

Genetic knockout of phosphoinositide 3-kinase (PI3K)γ (PI3K$\gamma^{-/-}$) in mice results in reduced phosphodiesterase activity, increased intracellular cAMP levels, and enhanced ventricular contractility.[1–5] We have previously demonstrated that increased contractility in ventricular myocytes isolated from PI3K$\gamma^{-/-}$ mice is attributable to elevated sarcoplasmic reticulum (SR) Ca^{2+} levels and increased SR Ca^{2+} release without changes in L-type Ca^{2+} current ($I_{Ca,L}$).[4,6] These results establish that the regulation of cAMP by PI3Kγ in ventricular myocytes occurs in a subcellular compartment containing the SR, but not L-type Ca^{2+} channels.[7]

Heart rate is determined by the electrical properties of specialized myocytes located in the sinoatrial node (SAN).[8,9] The spontaneous electrical activity of SAN myocytes results from slow diastolic depolarizations that increase the membrane potential toward the threshold for eliciting action potentials (APs). The activity of several currents involved in the regulation of spontaneous AP firing in SAN myocytes are modulated by cAMP, including the hyperpolarization-activated current (I_f), $I_{Ca,L}$, a delayed rectifier K^+ current (I_{Kr}) and a Na^+– Ca^{2+} exchange current (I_{NCX}) that is driven by SR Ca^{2+} release.[8–14] Because PI3Kγ has emerged as an important regulator of cAMP in the myocardium, and because cAMP is a critical modulator of SAN pacemaker cell activity, we sought to evaluate the role of PI3Kγ in heart rate regulation using transgenic mice lacking PI3Kγ. Our results indicate that PI3Kγ modulates the intrinsic activity of the SAN in a cAMP-dependent fashion and that the effects of PI3Kγ ablation in the SAN are unique compared with the working myocardium of the atria and ventricles. Some of these data have been presented in abstract form.[15]

Materials and Methods

Animals

In the present study, male wild-type (PI3K$\gamma^{+/+}$) and PI3K$\gamma^{-/-}$[16] littermate mice aged 10 to 14 weeks were used. All experimental procedures were in accordance with the regulations of The Canadian Council on Animal Care and were approved by the University of Toronto animal care facility.

In Vivo Heart Rate Measurements

Heart rate was measured in anesthetized mice using a pressure catheter (Millar Instruments) inserted into the aorta via the carotid artery, as described in the online data supplement at http://circres.ahajournals.org.

Original received June 21, 2007; revision received October 10, 2007; accepted October 19, 2007.

From the Departments of Physiology and Medicine (R.A.R., P.H.B.), Division of Cardiology at the University Health Network (R.A.R., P.H.B.), and Heart and Stroke/Richard Lewar Centre of Excellence (R.A.R., M.G.K., P.H.B.), University of Toronto, Ontario, Canada.

Correspondence to Dr Peter H. Backx, University of Toronto, Heart & Stroke/ Richard Lewar Centre, Room 68, Fitzgerald Building, 150 College St, Toronto, Ontario, Canada M5S 3E2. E-mail p.backx@utoronto.ca

Circulation Research **is available at http://circres.ahajournals.org** **DOI: 10.1161/CIRCRESAHA.107.158428**

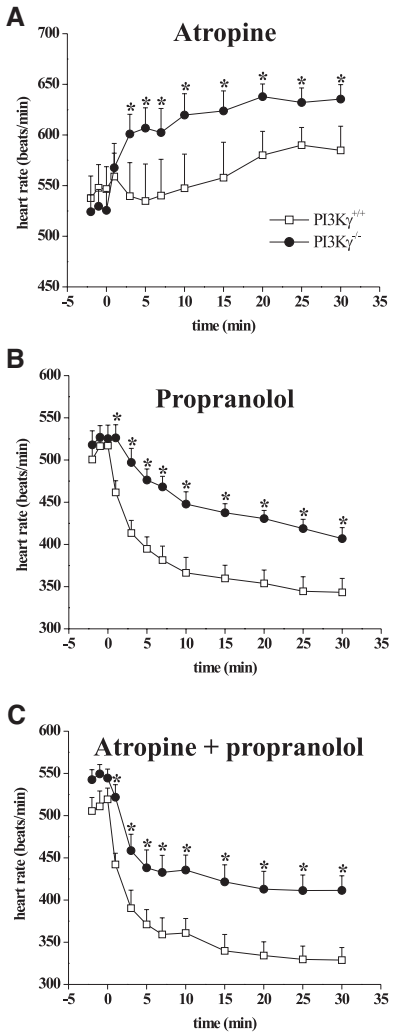

Figure 1. Effects of PI3Kγ ablation on heart rate in anesthetized mice under basal conditions and following nervous system blockade. Effect of atropine (1 mg/kg) (A), propranolol (1 mg/kg) (B), and a combination of atropine and propranolol (C) on heart rate in PI3K$\gamma^{+/+}$ and PI3K$\gamma^{-/-}$ mice. Drugs were give by IP injection at 0 minutes. Following all 3 pharmacological interventions, heart rate was significantly greater (*) in PI3K$\gamma^{-/-}$ mice than wild-type controls (n=6 to 7 mice for each test group).

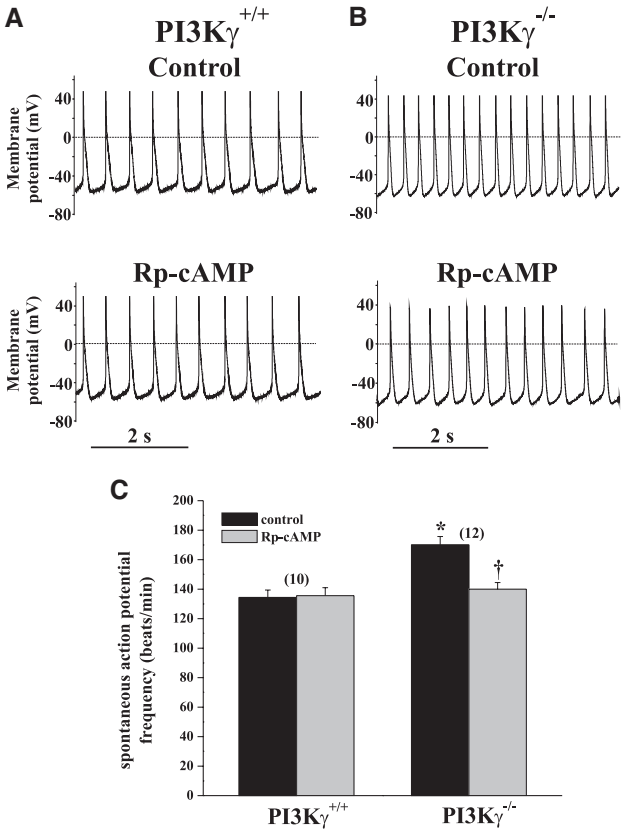

Figure 2. Effects of PI3Kγ ablation on spontaneous AP frequency in isolated SAN myocytes. A and B, Representative recordings of spontaneous APs in control conditions and following application of the cAMP/PKA antagonist Rp-cAMP (1×10^{-4} mol/L) in PI3K$\gamma^{+/+}$ and PI3K$\gamma^{-/-}$ myocytes. Recordings were made using the whole-cell configuration of the patch-clamp technique, and Rp-cAMP was included in the recording pipette, so that it could enter the cells by diffusion. C, Summary data demonstrating that spontaneous AP frequency was elevated in PI3K$\gamma^{-/-}$ myocytes in a cAMP/PKA-dependent fashion. *$P<0.05$ between genotypes under the same conditions. †$P<0.05$ for Rp-cAMP vs control within genotypes; n values in parentheses. Measurements were performed at room temperature (22°C to 23°C).

Isolation of Mouse SAN and Right Atrial Myocytes

The procedures for isolating single pacemaker myocytes from the SAN, as well as working right atrial myocytes from the mouse have been described[17–19] and are available in the online data supplement. Single SAN and right atrial myocytes were used for patch-clamp studies using standard solutions and electrophysiological protocols, which are detailed in the online data supplement.

Results

Consistent with previous reports,[1–3] no differences in heart rate were observed between PI3K$\gamma^{-/-}$ and PI3K$\gamma^{+/+}$ mice in control conditions (Figure 1). To assess whether the intrinsic electrical properties of the SAN differed between PI3K$\gamma^{-/-}$ and PI3K$\gamma^{+/+}$ mice, heart rate was also measured following selective blockade of the autonomic nervous system. Figure 1A shows that administration of atropine (1 mg/kg) to block parasympathetic nervous system activity caused heart rate to increase ($P<0.05$) from 544.1±22.2 to 589.9±17.5 beats per minute (bpm) over 20 minutes in PI3K$\gamma^{+/+}$ mice and from 526.4±17.3 to 635.4±14.3 bpm over shorter periods (≈5 minutes) in PI3K$\gamma^{-/-}$ mice. After atropine treatment, heart rate was higher ($P<0.05$) in PI3K$\gamma^{-/-}$ than PI3K$\gamma^{+/+}$ mice. Treatment with propranolol (1 mg/kg; Figure 1B) to block sympathetic nervous system activity reduced ($P<0.05$) heart rate in PI3K$\gamma^{+/+}$ (511.2±9.8 to 343.3±16.5 bpm) and PI3K$\gamma^{-/-}$ (523.4±15.5 to 406.9±13.0 bpm) mice. Following propranolol treatment, heart rate was greater ($P<0.05$) in PI3K$\gamma^{-/-}$ than PI3K$\gamma^{+/+}$ mice. Combined treatment with atropine and propranolol (Figure 1C) produced heart rate changes that were comparable to the effects of propranolol alone.

Because the results above suggest that PI3Kγ modulates the intrinsic pacemaker properties of the SAN, we directly assessed the electrical properties of isolated SAN myocytes. Spontaneous APs could be continuously recorded for at least 20 minutes and, as summarized in Figure 2, occurred at a

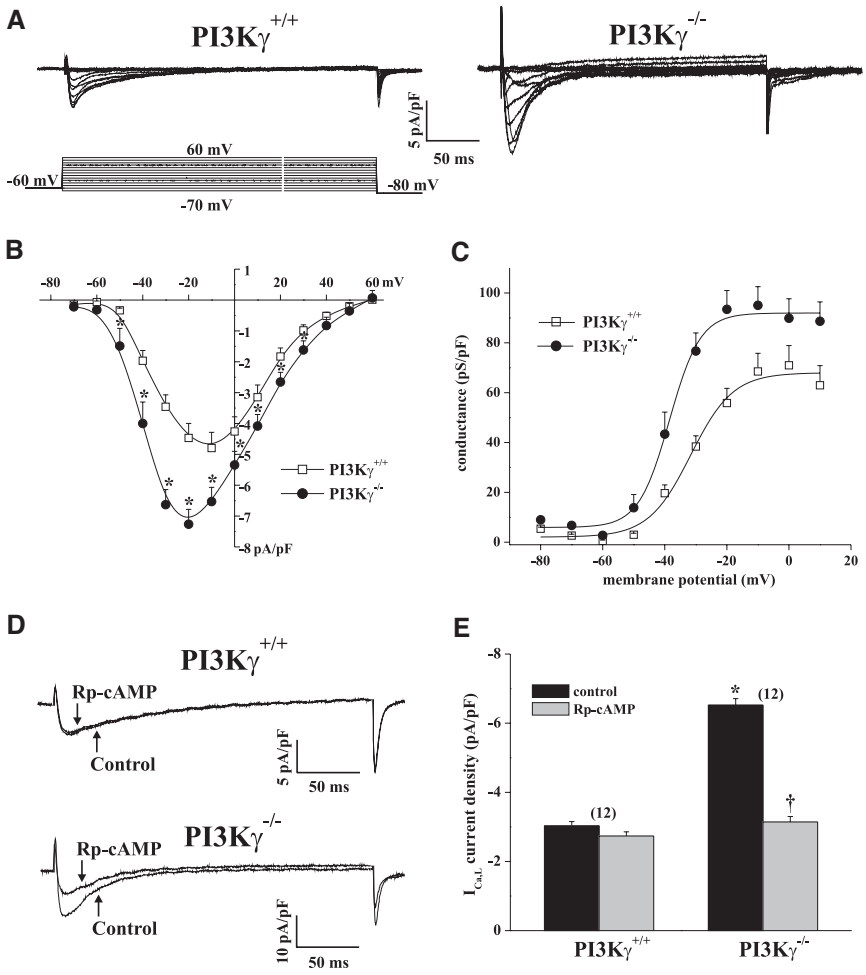

Figure 3. Effects of PI3Kγ ablation on $I_{Ca,L}$ in SAN myocytes. A, Representative current recordings of SAN $I_{Ca,L}$ in myocytes from PI3Kγ$^{+/+}$ and PI3Kγ$^{-/-}$ mice. B, Summary I-V curves demonstrating that SAN $I_{Ca,L}$ current density was elevated in PI3Kγ$^{-/-}$ mice (n=26 myocytes) compared with wild-type controls (n=21 myocytes). *$P<0.05$ at the given membrane potential. C, Activation curves for $I_{Ca,L}$ conductance in SAN myocytes demonstrating that G_{max} was elevated and $V_{1/2}$ of activation was left shifted in PI3Kγ$^{-/-}$ SAN myocytes compared with wild-type SAN myocytes (see text for details). D, Representative $I_{Ca,L}$ recordings (250-ms voltage-clamp step to −10 mV) in SAN myocytes from PI3Kγ$^{+/+}$ mice and PI3Kγ$^{-/-}$ mice before and after application of Rp-cAMP (1×10^{-4} mol/L). E, Summary data for the effects of Rp-cAMP on peak $I_{Ca,L}$. *$P<0.05$ between genotypes under the same conditions, †$P<0.05$ for Rp-cAMP vs control within the same genotype (n values in parentheses).

higher frequency ($P<0.05$) in PI3Kγ$^{-/-}$ myocytes (173±8 bpm) than PI3Kγ$^{+/+}$ myocytes (129±6 bpm). The relative differences in SAN myocyte firing rate between PI3Kγ$^{-/-}$ and PI3Kγ$^{+/+}$ were similar to the heart rate differences observed in mice following autonomic blockade, although the absolute rates differed because of temperature differences between the studies. These changes in AP frequency were associated with increases ($P<0.05$) in the slope of the diastolic depolarization (DD) from 25.1±1.5 mV/sec in PI3Kγ$^{+/+}$ myocytes to 41.7±1.4 mV/sec in PI3Kγ$^{-/-}$ myocytes, without changes ($P=0.62$) in the maximum diastolic potential between genotypes (supplemental Table I). Because the modulation of ventricular cardiomyocyte contractility by PI3Kγ depends on cAMP,[2,4] we examined the effects of the cAMP/protein kinase (PKA) antagonist adenosine-3′,5′ cyclic phosphorothioate (Rp-cAMP; 1×10^{-4} mol/L)[20] on SAN myocytes. Eight minutes of treatment with Rp-cAMP had no effect ($P=0.69$) on spontaneous AP frequency in PI3Kγ$^{+/+}$ SAN myocytes but reduced ($P<0.05$) firing frequency from 170±6 to 140±4 bpm and the DD slope from 48.9±3.5 to 22.2±1.2 mV/S in PI3Kγ$^{-/-}$ SAN myocytes, without affecting the maximum diastolic potential (Figure 2 and supplemental Table I). Firing frequencies were identical between the groups after Rp-cAMP.

To explore the ionic basis for the changes in AP-firing frequency, we measured $I_{Ca,L}$ and I_f because these currents alter the spontaneous firing rate of SAN myocytes in a cAMP-dependent manner by influencing the DD slope. Figure 3 shows representative $I_{Ca,L}$ recordings, originating from $Ca_V1.2$ and $Ca_V1.3$ channels, measured with voltage-clamp protocols designed to minimize T-type Ca^{2+} currents.[21] These recordings were done in the presence of tetrodotoxin (3×10^{-5} mol/L) or QX-314 (3×10^{-2} mol/L) to block voltage-gated Na^+ channels. $I_{Ca,L}$ current densities were larger ($P<0.05$), and the peak of the current–voltage relationship (I-V) curve was shifted toward negative potentials in PI3Kγ$^{-/-}$ versus PI3Kγ$^{+/+}$ SAN myocytes. Note that these I-V curves peak at more negative membrane potentials than ventricular myocytes because of the functional expression of the $Ca_V1.3$ channel isoform.[21] To better quantify the differences in $I_{Ca,L}$ between the groups, steady-state conductance analysis was performed, which revealed that the maximum conductance (G_{max}) was elevated ($P<0.05$) in PI3Kγ$^{-/-}$ (93.5±7.5 pS/pF) compared with PI3Kγ$^{+/+}$ (72.7±7.9 pS/pF) SAN myocytes (Figure 3C). Furthermore, the voltage required for 50% channel activation ($V_{1/2}$) was shifted ($P<0.05$) leftward from −30.6±1.7 mV for PI3Kγ$^{+/+}$ SAN myocytes to −38.5±2.0 mV in PI3Kγ$^{-/-}$ SAN myocytes (Figure 3C). Despite clear differences in channel activation, no differences ($P=0.89$) in the time constants for $I_{Ca,L}$ inactivation (ie, τ_{fast} and τ_{slow}) were observed between genotypes (supplemental Figure I). These changes in channel activation are expected to increase depo-

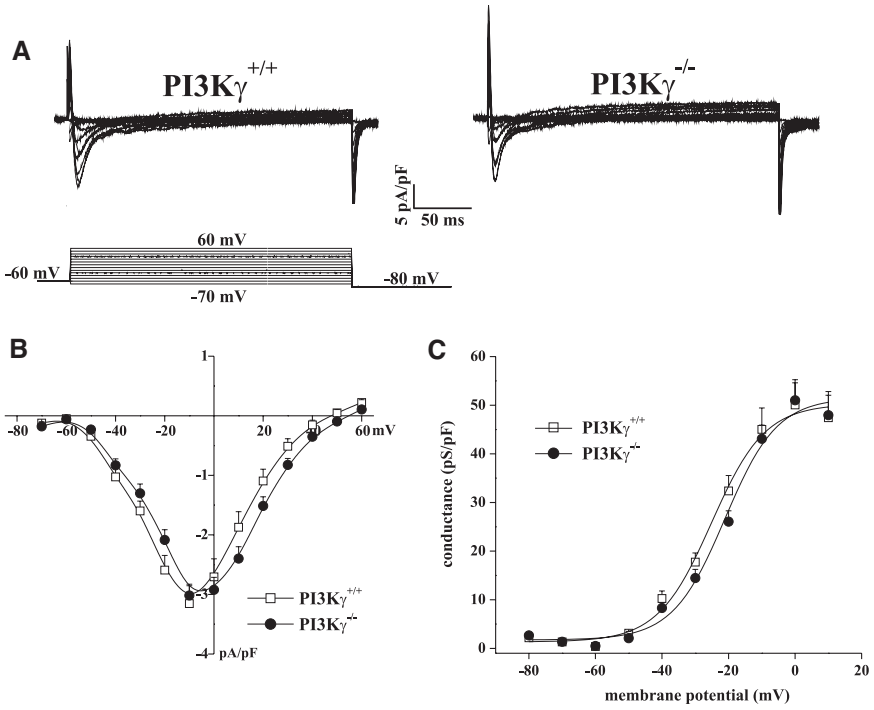

Figure 4. Effects of PI3Kγ ablation on $I_{Ca,L}$ in right atrial working myocytes. A, Representative $I_{Ca,L}$ recordings in right atrial myocytes from wild-type and PI3Kγ$^{-/-}$ mice. B and C, Summary I-V and activation curves showing that $I_{Ca,L}$ current density, G_{max}, and activation kinetics in right atrial myocytes were not significantly different between genotypes (n=17 PI3Kγ$^{+/+}$ myocytes and n=19 PI3Kγ$^{-/-}$ myocytes).

larizing currents leading to increased DD slopes and spontaneous firing frequencies.

Because the increase in G_{max} and the shift in $V_{1/2}$ for $I_{Ca,L}$ in PI3Kγ$^{-/-}$ SAN myocytes are reminiscent of changes observed following activation of cAMP/PKA in the myocardium, we examined the effects of the cAMP/PKA antagonist Rp-cAMP (1×10^{-4} mol/L) on $I_{Ca,L}$ measured at −10 mV, a voltage at which the conductance is maximal. As summarized in Figure 3D and 3E, Rp-cAMP had no effect ($P=0.30$) on $I_{Ca,L}$ in PI3Kγ$^{+/+}$ SAN myocytes but reduced ($P<0.05$) peak $I_{Ca,L}$ in PI3Kγ$^{-/-}$ to levels not different from PI3Kγ$^{+/+}$ myocytes in the presence or absence of Rp-cAMP. Similarly, Rp-cAMP had no effect ($P=0.12$) on G_{max} or $V_{1/2}$ of activation for $I_{Ca,L}$ in PI3Kγ$^{+/+}$ SAN myocytes but reduced ($P<0.05$) G_{max} and shifted $V_{1/2}$ in PI3Kγ$^{-/-}$ SAN myocytes to values that were not different ($P=0.48$) from PI3Kγ$^{+/+}$ (supplemental Figure II).

The cAMP-dependent $I_{Ca,L}$ elevations in PI3Kγ$^{-/-}$ SAN myocytes contrasts with the lack of effect of PI3Kγ ablation on $I_{Ca,L}$ in ventricular myocytes.[4] Because $I_{Ca,L}$ is only produced by $Ca_V1.2$ channels in ventricular myocytes, but is generated by $Ca_V1.2$ and $Ca_V1.3$ channels in SAN myocytes, we considered the possibility that $I_{Ca,L}$ elevations in PI3Kγ$^{-/-}$ SAN myocytes originate from cAMP-dependent regulation of $Ca_V1.3$ channels. To test this possibility, we took advantage of the fact that, like SAN myocytes, working atrial myocytes also express $Ca_V1.2$ and $Ca_V1.3$ L-type Ca^{2+} channels.[21–23] As summarized in Figure 4 (and supplemental Figure I), $I_{Ca,L}$ in right atrial myocytes did not differ ($P=0.85$) between PI3Kγ$^{+/+}$ and PI3Kγ$^{-/-}$, suggesting that increased $I_{Ca,L}$ in PI3Kγ$^{-/-}$ SAN myocytes is unlikely to result from distinct regulation of $Ca_V1.3$ L-type Ca^{2+} channels by PI3Kγ.

Next, we recorded I_f. Our data illustrate that I_f current density was higher ($P<0.05$) in PI3Kγ$^{-/-}$ SAN myocytes, compared with PI3Kγ$^{+/+}$ myocytes, at membrane potentials less than or equal to −80 mV (Figure 5). These elevated current densities were accompanied by a shift ($P<0.05$) in the $V_{1/2}$ for channel activation (−96.4±1.0 mV for PI3Kγ$^{+/+}$ myocytes versus −88.5±0.9 mV for PI3Kγ$^{-/-}$ myocytes) with no change ($P=0.14$) in slope factor (18.5±0.9 for PI3Kγ$^{-/-}$ versus 19.0±0.8 for PI3Kγ$^{+/+}$). These differences in I_f are anticipated to increase depolarizing currents, leading to a higher DD slopes and firing rates in PI3Kγ$^{-/-}$ myocytes.

To determine whether these I_f differences resulted from altered cAMP/PKA signaling between the groups, the effects of Rp-cAMP (1×10^{-4} mol/L) were examined (Figure 6A and 6B). In these studies, the control current levels were measured 30 seconds after rupturing the cell membrane, and the effects of Rp-cAMP were measured after 8 minutes of dialysis (see Materials and Methods). Rp-cAMP increased ($P<0.05$) I_f (at −120 mV) slightly from −10.2±0.8 to −11.9±0.9 pA/pF in PI3Kγ$^{+/+}$ SAN myocytes while reducing ($P<0.05$) I_f from −18.4±0.8 to −15.7±1.2 pA/pF in PI3Kγ$^{-/-}$ SAN myocytes. The ability of Rp-cAMP to increase I_f in PI3Kγ$^{+/+}$ SAN myocytes is not unexpected because, whereas Rp-cAMP can block PKA activation, it also directly activates hyperpolarization-activated, cyclic nucleotide–gated (HCN) channels.[24,25] Thus, to dissect the contributions of PKA to the enhanced I_f in PI3Kγ$^{-/-}$, myocytes were dialyzed with a 14-22-amide protein kinase inhibitor (PKI_{14-22}) (1×10^{-5} mol/L), which is the inhibitor peptide for the PKA catalytic subunit.[26] PKI_{14-22} had no effect on I_f in PI3Kγ$^{+/+}$ SAN myocytes, but caused I_f reductions in PI3Kγ$^{-/-}$ SAN myocytes similar to those seen with Rp-cAMP (Figure 6C and 6D).

The results above establish that increased spontaneous firing rates of SAN myocytes in PI3Kγ$^{-/-}$ mice are related to elevated cAMP/PKA signaling. To explore cAMP signaling

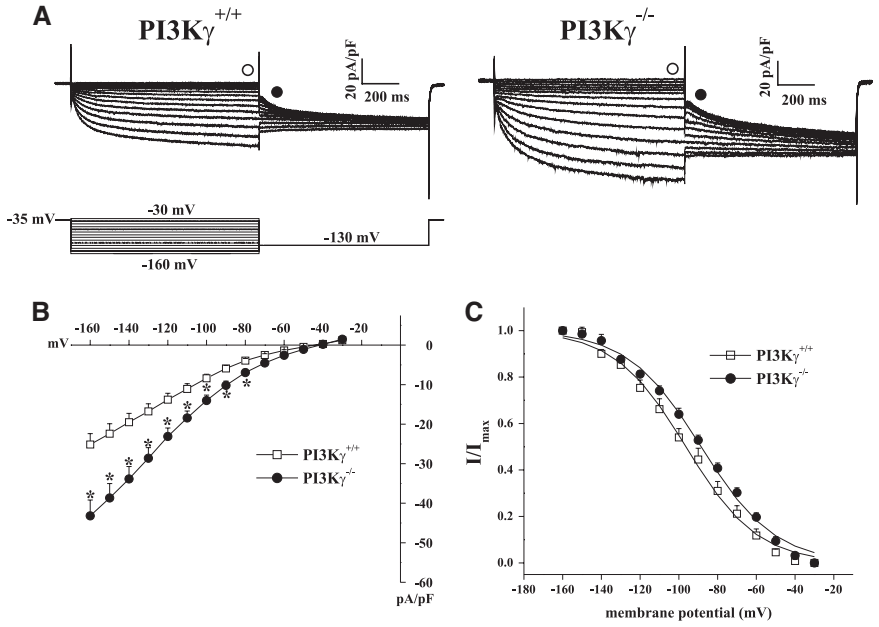

Figure 5. Properties of I_f in SAN myocytes from PI3K$\gamma^{-/-}$ mice. A, Representative I_f recordings from wild-type and knockout myocytes. B, Summary I-V curves (measured at the time point indicated by the open circles in (A) demonstrating that I_f is increased in PI3K$\gamma^{-/-}$ mice (n=19 myocytes) compared with PI3K$\gamma^{+/+}$ mice (n=22 myocytes). *$P<0.05$ at the given membrane potential. C, I_f activation curves in wild-type and PI3K$\gamma^{-/-}$ mice, which were measured at the points indicated by black circles in A. $V_{1/2}$ was significantly shifted to the right in PI3K$\gamma^{-/-}$ mice (n=14 myocytes) compared with PI3K$\gamma^{+/+}$ mice (n=15 myocytes).

further, we investigated the effects of isoproterenol (ISO). As expected, application of ISO (1×10^{-6} mol/L) increased ($P<0.05$) AP frequency from 118±9 to 154±6 bpm in PI3K$\gamma^{+/+}$ myocytes (Figure 7A and 7B), in association with increases ($P<0.05$) in DD slope, AP overshoot, and AP duration measured at 50% repolarization (APD_{50}) (supplemental Table I). In PI3K$\gamma^{-/-}$ myocytes, ISO application increased ($P<0.05$) AP frequency from 183±6 to 207±6 bpm with relatively similar changes in AP profile, as seen in PI3K$\gamma^{+/+}$ SAN myocytes (Figure 7B and supplemental Table I), establishing that cAMP-dependent signaling is not saturated under baseline conditions in PI3K$\gamma^{-/-}$ SAN myocytes. Indeed, both $I_{Ca,L}$ and I_f were increased ($P<0.05$) by β-adrenergic receptor stimulation with ISO in PI3K$\gamma^{-/-}$ and PI3K$\gamma^{+/+}$ SAN myocytes (Figure 7C through 7F).

SAN pacemaker activity has been shown to be modulated by SR Ca^{2+} loading and release,[14,27,28] which are both regulated by cAMP/PKA and markedly increased in PI3K$\gamma^{-/-}$ ventricular myocytes.[4,5] Therefore, we tested the effects of the SR Ca^{2+} release blocker ryanodine (1×10^{-5} mol/L) on spontaneous AP frequency. Representative AP recordings in control conditions and after treatment with ryanodine (minimum 8 minutes; Figure 8) show firing frequency was reduced ($P<0.05$) by approximately the same percentage in PI3K$\gamma^{-/-}$

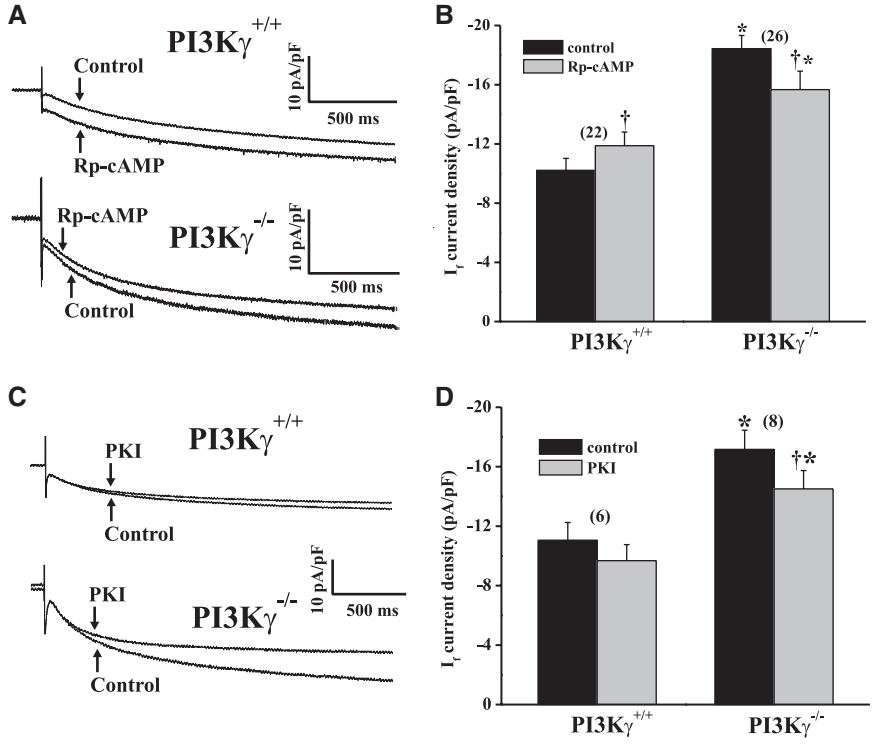

Figure 6. Effects of Rp-cAMP and PKI_{14-22} on I_f in SAN myocytes from wild-type and PI3K$\gamma^{-/-}$ mice. A, Representative I_f recordings (2-second voltage-clamp step to −120 mV) in myocytes from PI3K$\gamma^{+/+}$ mice and PI3K$\gamma^{-/-}$ mice before and after treatment with Rp-cAMP (1×10^{-4} mol/L). B, Summary data for the effects of Rp-cAMP on I_f. C, Representative I_f recordings before and after treatment with PKI_{14-22}. D, Summary data for the effects of PKI_{14-22} of I_f. *$P<0.05$ between genotypes under the same conditions, †$P<0.05$ for Rp-cAMP vs control within the same genotype (n values in parentheses).

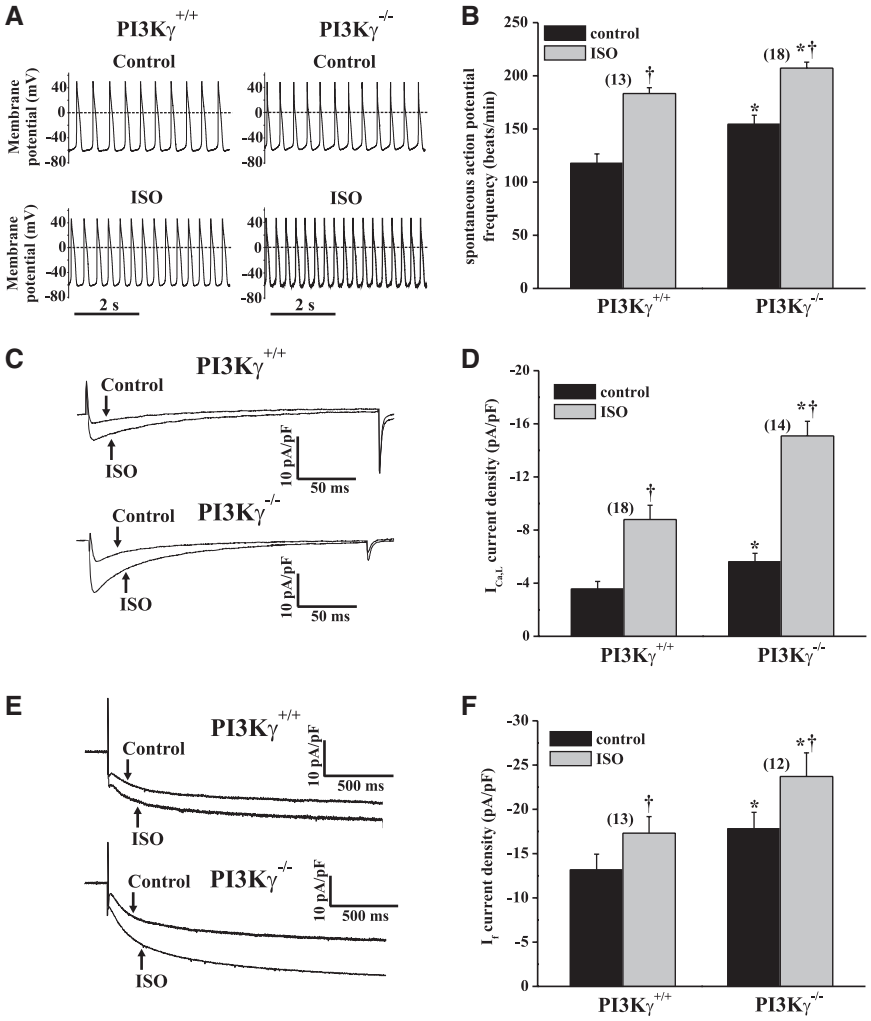

Figure 7. Effects of ISO on spontaneous AP firing, $I_{Ca,L}$, and I_f in SAN myocytes from wild-type and PI3K$\gamma^{-/-}$ mice. A, Representative recordings of spontaneous APs in control conditions and following the application of the β-adrenergic receptor agonist ISO (1×10^{-6} mol/L) for 5 minutes in PI3K$\gamma^{+/+}$ and PI3K$\gamma^{-/-}$ SAN myocytes. Summary data are illustrated in B. C, Representative $I_{Ca,L}$ recordings during a 250-ms voltage-clamp step to −10 mV in control conditions and after superfusion with ISO with summary data shown in D. E, Representative I_f recordings during a 2-second voltage-clamp step to −120 mV before and after superfusion with ISO. Summary data for I_f are shown in F. *$P<0.05$ between genotypes under the same conditions. †$P<0.05$ for ISO vs control within genotypes (n values in parentheses).

SAN myocytes (166±11 to 131±8 bpm) as in PI3K$\gamma^{+/+}$ SAN myocytes (135±5 to 105±6 bpm). Ryanodine also reduced ($P<0.05$) DD slope and increased ($P<0.05$) APD_{50} (supplemental Table I). Thus, AP-firing frequencies remained elevated ($P<0.05$) in PI3K$\gamma^{-/-}$ SAN myocytes after inhibition of SR Ca^{2+} release, suggesting that differences in SR function are not responsible for the higher firing rates in PI3K$\gamma^{-/-}$ SAN myocytes.

Heart rate is also potently regulated by parasympathetic nervous system-mediated stimulation of M2 muscarinic receptors in the SAN, which activate hyperpolarizing acetylcholine-sensitive K^+ currents (I_{KACh}) via $G_{\beta\gamma}$ subunits.[29] Because heart rate (Figure 1) differed between PI3K$\gamma^{+/+}$ and PI3K$\gamma^{-/-}$ mice after autonomic blockade, we also examined I_{KACh} in SAN myocytes. I_{KACh} evoked by carbachol (1×10^{-5} mol/L)[17] did not differ between PI3K$\gamma^{+/+}$ and PI3K$\gamma^{-/-}$ SAN myocytes (supplemental Figure III), indicating that the properties of I_{KACh} are not directly affected by PI3Kγ.

Discussion

Although our studies demonstrate that PI3Kγ negatively regulates the spontaneous firing rate of isolated SAN myocytes, heart rate was not different between wild-type and PI3K$\gamma^{-/-}$ mice under basal conditions. This is not unexpected because heart rate in vivo is regulated by the autonomic nervous system.[30,31] Indeed, blockade of the sympathetic or parasympathetic arms of the autonomic nervous system unmasked elevated heart rates in PI3K$\gamma^{-/-}$ mice with the relative heart rate differences after combined propranolol and atropine treatment being similar to the relative differences in spontaneous firing rate observed in isolated SAN myocytes. Interestingly, whereas both propranolol and atropine treatment affected heart rate, sympathetic blockade had a relatively larger effect in agreement with previous mouse studies.[32–34] Furthermore, the larger heart rate changes with atropine in PI3K$\gamma^{-/-}$ (compared with PI3K$\gamma^{+/+}$) mice suggest that elevated parasympathetic activity is used by PI3K$\gamma^{-/-}$ mice to suppress higher intrinsic AP rates of their SANs, even though I_{KACh} was not directly affected by PI3Kγ.

Consistent with previous reports showing that PI3Kγ is a negative regulator of cAMP in the ventricular myocardium,[1–3] we found that the cAMP/PKA blocker Rp-cAMP reduced AP firing frequency in PI3K$\gamma^{-/-}$ SAN myocytes to levels indistinguishable from PI3K$\gamma^{+/+}$ SAN myocytes in the absence or presence of Rp-cAMP. The differences in AP firing observed between PI3K$\gamma^{+/+}$ and PI3K$\gamma^{-/-}$ SAN myocytes, as well as the changes induced by Rp-cAMP, correlated tightly with changes in the slope of the DD. Under

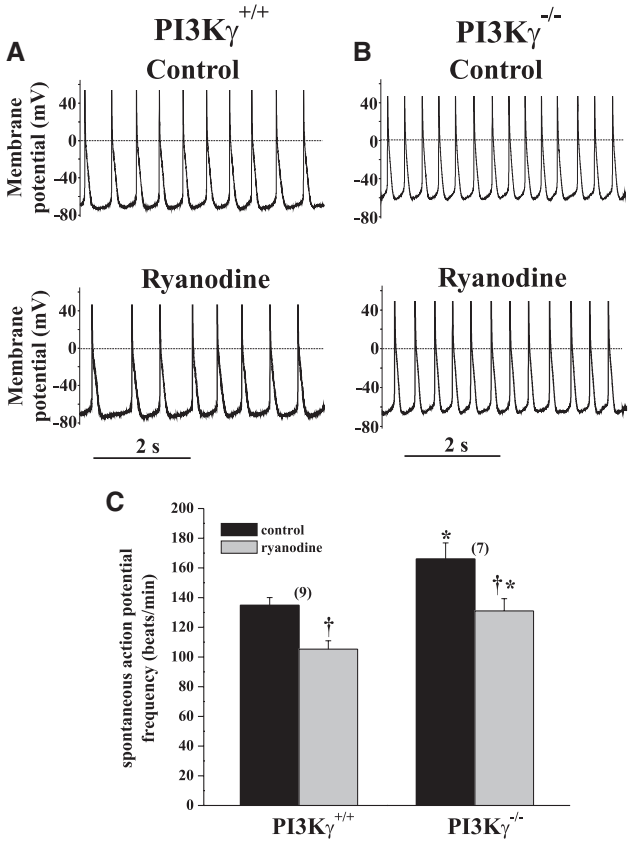

Figure 8. Effects of ryanodine on spontaneous AP firing in SAN myocytes from wild-type and PI3K$\gamma^{-/-}$ mice. A and B, Representative recordings of spontaneous APs in control conditions and following the application of ryanodine (1×10^{-5} mol/L). C, Summary data demonstrating that AP-firing frequency was reduced in both genotypes following treatment with ryanodine. *$P<0.05$ between genotypes under the same conditions, †$P<0.05$ for ryanodine vs control within genotypes (n values in parentheses).

physiological conditions, several channels whose activities are increased by β-adrenergic receptor-mediated elevations in cAMP/PKA signaling provide depolarizing current during the diastolic period.

$I_{Ca,L}$ is an attractive candidate to explain the differences in spontaneous AP firing between PI3K$\gamma^{+/+}$ and PI3K$\gamma^{-/-}$ SAN myocytes and the response to Rp-cAMP in PI3K$\gamma^{-/-}$ SAN myocytes, for several reasons. First, $I_{Ca,L}$ in SAN myocytes is generated by 2 distinct L-type Ca^{2+} channel α1 subunits: $Ca_V1.2$ and $Ca_V1.3$. Whereas $Ca_V1.2$ channels contribute primarily to the AP upstroke, $Ca_V1.3$ channels activate at more negative membrane potentials that correspond to the late phase of the DD in SAN myocytes.[21,22] Second, $I_{Ca,L}$ was increased in PI3K$\gamma^{-/-}$ SAN myocytes because of an increased conductance (G_{max}) and a leftward shift in $V_{1/2}$ for channel activation, changes that mimic the alterations seen with β-adrenergic receptor–mediated elevations in cAMP/PKA signaling. The leftward shift in $V_{1/2}$ preferentially increases $I_{Ca,L}$ at potentials corresponding to the DD. Third, the effects of Rp-cAMP on $I_{Ca,L}$ closely mirrored the effects on spontaneous firing rates. Specifically, the elevation in $I_{Ca,L}$ density that was observed in PI3K$\gamma^{-/-}$ SAN myocytes was eliminated by Rp-cAMP. On the other hand, Rp-cAMP had no effect on $I_{Ca,L}$ in PI3K$\gamma^{+/+}$ SAN myocytes. Thus, our findings suggest that cAMP-dependent regulation of $I_{Ca,L}$ is a major determinant of the firing rate of the mouse SAN, as concluded previously.[19,21] Consistent with this suggestion, $I_{Ca,L}$ is a prototype for cAMP/PKA-dependent phosphorylation,[35,36] and $I_{Ca,L}$ blockers are routinely used in the effective treatment of atrial tachyarrhythmias.[37] It could be hypothesized that the negative shift in $I_{Ca,L}$ activation properties (ie, $V_{1/2}$) between genotypes results from an increased role for $Ca_v1.3$ channels in PI3K$\gamma^{-/-}$ SAN myocytes. However, this seems unlikely because $V_{1/2}$ (as well as G_{max}) was identical between genotypes after Rp-cAMP addition.

Another potential contributor to the elevated AP-firing rates in PI3K$\gamma^{-/-}$ SAN myocytes is the "pacemaker current" I_f, even though the role of I_f in cardiac pacemaking has been challenged.[9] Careful analysis of our AP recordings reveal that the maximum diastolic potential in mouse SAN myocytes is approximately -60 mV for both genotypes. Because our I_f I-V curves revealed that the I_f density was not statistically different between PI3K$\gamma^{+/+}$ and PI3K$\gamma^{-/-}$ SAN myocytes at potentials above -80 mV, it could be concluded that I_f does not contribute to the rate differences between these genotypes. However, our I_f activation curve measurements reveal that voltages of approximately -60 mV are sufficiently positive to activate I_f in both genotypes, consistent with previous studies showing that I_f contributes to AP firing in mouse SAN.[18,38] More importantly, because $V_{1/2}$ is significantly shifted to more positive potentials and because the maximal I_f densities are increased, the degree of I_f activation is greater in PI3K$\gamma^{-/-}$ SAN myocytes at these diastolic voltages, suggesting that I_f differences can contribute to higher firing rates in PI3K$\gamma^{-/-}$ SAN myocytes. It is also conceivable that differences in I_f channel gating attributable to hysteresis, a property demonstrated in HCN channels,[39,40] which was not assessed in our studies, could increase the impact of I_f on SAN firing rates in the 2 genotypes.

Our results show that Rp-cAMP reduced I_f in PI3K$\gamma^{-/-}$ SAN myocytes but slightly increased I_f in wild-type myocytes. Moreover, I_f remained elevated in PI3K$\gamma^{-/-}$ SAN myocytes after Rp-cAMP treatment. These complex results can be understood by recognizing that Rp-cAMP can affect I_f in 2 ways. First, like cAMP and other cAMP analogs, Rp-cAMP can increase I_f by directly binding to HCN channels via a cyclic nucleotide binding domain.[10,25] On the other hand, I_f is also regulated by PKA-dependent phosphorylation,[41,42] consistent with the presence of several consensus PKA phosphorylation sites in HCN4 channels, the major HCN homolog in mouse SAN.[38,43] Thus, in PI3K$\gamma^{+/+}$ SAN myocytes Rp-cAMP addition is expected to enhance I_f by direct binding to the channels. By contrast, in PI3K$\gamma^{-/-}$ myocytes Rp-cAMP treatment is expected to inhibit PKA, thereby reducing I_f while simultaneously adding to the elevated cAMP pool, which results in elevations of I_f above those seen in wild-type SAN. Consistent with this interpretation, PKA inhibition with PKI_{14-22} had no affect on I_f in PI3K$\gamma^{+/+}$ SAN myocytes but reduced I_f in PI3K$\gamma^{-/-}$ SAN to levels still exceeding wild-type mice, because of persistent cAMP elevations in PI3K$\gamma^{-/-}$ myocytes. These data suggest that elevated cAMP in PI3K$\gamma^{-/-}$ mice increases I_f both by

direct binding and by PKA-mediated effects. Furthermore, because Rp-cAMP in PI3K$\gamma^{-/-}$ mice did not reduce I_f to wild-type levels but did normalize firing rates, it appears that I_f differences make relatively minor contributions to the elevated AP-firing rates in PI3K$\gamma^{-/-}$ SAN.

Previous work from our laboratory demonstrated that ventricular myocytes from PI3K$\gamma^{-/-}$ mice have large increases in SR Ca^{2+} cycling.[7] Because SR Ca^{2+} cycling has been shown to be an important modulator of spontaneous firing rates of SAN myocytes, we tested the effects of ryanodine on these myocytes at doses that block SR Ca^{2+} release.[27] Ryanodine reduced AP-firing frequency by ≈20% in both genotypes, confirming a role for the SR in pacemaker function in the mouse SAN. Importantly, after ryanodine treatment, AP firing continued in both genotypes and remained significantly elevated in PI3K$\gamma^{-/-}$ SAN myocytes, although a greater beat-to-beat variability in AP-firing pattern was observed in the wild-type mice as described previously.[44] These data, together with our voltage-clamp results, support the conclusion that the elevated SAN firing rate of PI3Kγ knockout mice is primarily driven by increases in sarcolemmal currents, such as $I_{Ca,L}$ and possibly I_f, although contributions from changes in SR Ca^{2+} cycling cannot be fully ruled out.

Increased $I_{Ca,L}$ in PI3K$\gamma^{-/-}$ SAN myocytes is clearly distinct from the absence of differences in $I_{Ca,L}$ in PI3K$\gamma^{-/-}$ ventricular myocytes.[7] In the current study, we also observed no differences in $I_{Ca,L}$ density or activation kinetics between wild-type and PI3K$\gamma^{-/-}$ right atrial myocytes. Importantly, $Ca_V1.3$ channels are functional in working mouse atrial myocytes,[23] as well as SAN myocytes.[21,22] Therefore, if PI3Kγ were selectively regulating $Ca_V1.3$ channels, alterations in $I_{Ca,L}$ activation kinetics would be expected for the working right atrial myocytes in PI3K$\gamma^{-/-}$ mice, which was not observed. These results suggest that selective cAMP-dependent modulation of $Ca_V1.3$ versus $Ca_V1.2$ channels does not underlie the elevated $I_{Ca,L}$ in PI3K$\gamma^{-/-}$ SAN myocytes. Rather, our data support the conclusion that PI3Kγ is critical for the baseline suppression of cAMP levels in intracellular microdomains containing L-type Ca^{2+} channels in SAN myocytes but not in working atrial or ventricular myocytes. The basis for these differences between myocytes from different regions is unclear, but tight spatiotemporal regulation of cAMP in microdomains of cells appears to involve macromolecular complexes containing many players, including phosphodiesterases and A kinase anchoring proteins.[45–47] It is possible that PI3Kγ is differentially integrated into such macromolecular complexes in a regional-dependent manner in the heart.

Significance

SAN dysfunction is a major burden that progressively increases with age and in disease states. For example, bradyarrhythmias associated with sick sinus syndrome account for a large proportion of sudden deaths during heart failure.[30] The cause of SAN dysfunction in heart failure is unclear, but heart disease is associated with impaired β-adrenergic/cAMP/PKA signaling, as well as altered function of L-type Ca^{2+} channels in the SAN.[30,48] In the present study, we show that PI3Kγ profoundly modulates SAN function and heart rate and that this modulation is cAMP dependent. Previous studies have shown that PI3Kγ expression is strongly increased in disease[49]; therefore, it is possible that PI3Kγ may contribute to the onset and maintenance of bradyarrhythmias in heart disease, as well as to SAN dysfunction more generally.

Acknowledgments

We thank Dr Benoit-Gilles Kerfant for helpful discussions.

Sources of Funding

This work was supported by Canadian Institutes for Health Research funding (to P.H.B.). P.H.B. is a career investigator with the Heart and Stroke Foundation of Ontario. R.A.R. is the recipient of Postdoctoral fellowships from the Heart and Stroke Foundation of Canada, The Alberta Heritage Foundation for Medical Research, and the Canadian Institutes of Health Research Tailored Advanced Collaborative Training in Cardiovascular Science (TACTICS) program.

Disclosures

None.

References

1. Alloatti G, Marcantoni A, Levi R, Gallo MP, Del Sorbo L, Patrucco E, Barberis L, Malan D, Azzolino O, Wymann M, Hirsch E, Montrucchio G. Phosphoinositide 3-kinase γ controls autonomic regulation of the mouse heart through G_i-independent downregulation of cAMP level. *FEBS Lett*. 2005;579:133–140.
2. Crackower MA, Oudit GY, Kozieradzki I, Sarao R, Sun H, Sasaki T, Hirsch E, Suzuki A, Shioi T, Irie-Sasaki J, Sah R, Cheng HY, Rybin VO, Lembo G, Fratta L, Oliveira-dos-Santos AJ, Benovic JL, Kahn CR, Izumo S, Steinberg SF, Wymann MP, Backx PH, Penninger JM. Regulation of myocardial contractility and cell size by distinct PI3K-PTEN signaling pathways. *Cell*. 2002;110:737–749.
3. Patrucco E, Notte A, Barberis L, Selvetella G, Maffei A, Brancaccio M, Marengo S, Russo G, Azzolino O, Rybalkin SD, Silengo L, Altruda F, Wetzker R, Wymann MP, Lembo G, Hirsch E. PI3Kγ modulates the cardiac response to chronic pressure overload by distinct kinase-dependent and -independent effects. *Cell*. 2004;118:375–387.
4. Kerfant BG, Gidrewicz D, Sun H, Oudit GY, Penninger JM, Backx PH. Cardiac sarcoplasmic reticulum calcium release and load are enhanced by subcellular cAMP elevations in PI3Kγ-deficient mice. *Circ Res*. 2005; 96:1079–1086.
5. Kerfant BG, Zhao D, Lorenzen-Schmidt I, Wilson LS, Cai S, Chen SR, Maurice DH, Backx PH. PI3Kγ is required for PDE4, not PDE3, activity in subcellular microdomains containing the sarcoplasmic reticular calcium ATPase in cardiomyocytes. *Circ Res*. 2007;101:400–408.
6. Sun H, Kerfant BG, Zhao D, Trivieri MG, Oudit GY, Penninger JM, Backx PH. Insulin-like growth factor-1 and PTEN deletion enhance cardiac L-type Ca^{2+} currents via increased PI3Kα/PKB signaling. *Circ Res*. 2006;98:1390–1397.
7. Kerfant BG, Rose RA, Sun H, Backx PH. Phosphoinositide 3-kinase γ regulates cardiac contractility by locally controlling cyclic adenosine monophosphate levels. *Trends Cardiovasc Med*. 2006;16:250–256.
8. DiFrancesco D. Pacemaker mechanisms in cardiac tissue. *Annu Rev Physiol*. 1993;55:455–472.
9. Irisawa H, Brown HF, Giles W. Cardiac pacemaking in the sinoatrial node. *Physiol Rev*. 1993;73:197–227.
10. Accili EA, Proenza C, Baruscotti M, DiFrancesco D. From funny current to HCN channels: 20 years of excitation. *News Physiol Sci*. 2002;17: 32–37.
11. Cho HS, Takano M, Noma A. The electrophysiological properties of spontaneously beating pacemaker cells isolated from mouse sinoatrial node. *J Physiol*. 2003;550:169–180.
12. Clark RB, Mangoni ME, Lueger A, Couette B, Nargeot J, Giles WR. A rapidly activating delayed rectifier K^+ current regulates pacemaker activity in adult mouse sinoatrial node cells. *Am J Physiol*. 2004;286: H1757–H1766.

13. Rigg L, Terrar DA. Possible role of calcium release from the sarcoplasmic reticulum in pacemaking in guinea-pig sino-atrial node. *Exp Physiol*. 1996;81:877–880.
14. Vinogradova TM, Maltsev VA, Bogdanov KY, Lyashkov AE, Lakatta EG. Rhythmic Ca^{2+} oscillations drive sinoatrial nodal cell pacemaker function to make the heart tick. *Ann N Y Acad Sci*. 2005;1047:138–156.
15. Rose RA, Kabir MG, Backx PH. Phosphoinositide-3-kinase γ regulates heart rate in vivo and modulates membrane currents in isolated mouse sinoatrial node cells. *Circulation.* 2006;114(suppl II):II-291 Abstract.
16. Sasaki T, Irie-Sasaki J, Jones RG, Oliveira-dos-Santos AJ, Stanford WL, Bolon B, Wakeham A, Itie A, Bouchard D, Kozieradzki I, Joza N, Mak TW, Ohashi PS, Suzuki A, Penninger JM. Function of PI3Kγ in thymocyte development, T cell activation, and neutrophil migration. *Science*. 2000;287:1040–1046.
17. Lomax AE, Rose RA, Giles WR. Electrophysiological evidence for a gradient of G protein-gated K^+ current in adult mouse atria. *Br J Pharmacol*. 2003;140:576–584.
18. Mangoni ME, Nargeot J. Properties of the hyperpolarization-activated current (I_f) in isolated mouse sino-atrial cells. *Cardiovasc Res*. 2001;52:51–64.
19. Rose RA, Lomax AE, Kondo CS, Anand-Srivastava MB, Giles WR. Effects of C-type natriuretic peptide on ionic currents in mouse sinoatrial node: a role for the NPR-C receptor. *Am J Physiol*. 2004;286:H1970–H1977.
20. Rothermel JD, Parker Botelho LH. A mechanistic and kinetic analysis of the interactions of the diastereoisomers of adenosine 3′,5′-(cyclic)phosphorothioate with purified cyclic AMP-dependent protein kinase. *Biochem J*. 1988;251:757–762.
21. Mangoni ME, Couette B, Bourinet E, Platzer J, Reimer D, Striessnig J, Nargeot J. Functional role of L-type Cav1.3 Ca^{2+} channels in cardiac pacemaker activity. *Proc Natl Acad Sci U S A*. 2003;100:5543–5548.
22. Zhang Z, Xu Y, Song H, Rodriguez J, Tuteja D, Namkung Y, Shin HS, Chiamvimonvat N. Functional Roles of $Ca_v1.3$ (α_{1D}) calcium channel in sinoatrial nodes: insight gained using gene-targeted null mutant mice. *Circ Res*. 2002;90:981–987.
23. Zhang Z, He Y, Tuteja D, Xu D, Timofeyev V, Zhang Q, Glatter KA, Xu Y, Shin HS, Low R, Chiamvimonvat N. Functional roles of $Ca_v1.3(\alpha_{1D})$ calcium channels in atria: insights gained from gene-targeted null mutant mice. *Circulation*. 2005;112:1936–1944.
24. Bois P, Renaudon B, Baruscotti M, Lenfant J, DiFrancesco D. Activation of f-channels by cAMP analogues in macropatches from rabbit sino-atrial node myocytes. *J Physiol*. 1997;501:565–571.
25. DiFrancesco D, Tortora P. Direct activation of cardiac pacemaker channels by intracellular cyclic AMP. *Nature*. 1991;351:145–147.
26. Vinogradova TM, Lyashkov AE, Zhu W, Ruknudin AM, Sirenko S, Yang D, Deo S, Barlow M, Johnson S, Caffrey JL, Zhou YY, Xiao RP, Cheng H, Stern MD, Maltsev VA, Lakatta EG. High basal protein kinase A-dependent phosphorylation drives rhythmic internal Ca^{2+} store oscillations and spontaneous beating of cardiac pacemaker cells. *Circ Res*. 2006;98:505–514.
27. Bogdanov KY, Vinogradova TM, Lakatta EG. Sinoatrial nodal cell ryanodine receptor and Na^+-Ca^{2+} exchanger: molecular partners in pacemaker regulation. *Circ Res*. 2001;88:1254–1258.
28. Bucchi A, Baruscotti M, Robinson RB, DiFrancesco D. I_f-dependent modulation of pacemaker rate mediated by cAMP in the presence of ryanodine in rabbit sino-atrial node cells. *J Mol Cell Cardiol*. 2003;35:905–913.
29. Wickman K, Clapham DE. Ion channel regulation by G proteins. *Physiol Rev*. 1995;75:865–885.
30. Dobrzynski H, Boyett MR, Anderson RH. New insights into pacemaker activity: promoting understanding of sick sinus syndrome. *Circulation*. 2007;115:1921–1932.
31. de Marneffe M, Gregoire JM, Waterschoot P, Kestemont MP. The sinus node and the autonomic nervous system in normals and in sick sinus patients. *Acta Cardiol*. 1995;50:291–308.
32. Gehrmann J, Hammer PE, Maguire CT, Wakimoto H, Triedman JK, Berul CI. Phenotypic screening for heart rate variability in the mouse. *Am J Physiol*. 2000;279:H733–H740.
33. Jumrussirikul P, Dinerman J, Dawson TM, Dawson VL, Ekelund U, Georgakopoulos D, Schramm LP, Calkins H, Snyder SH, Hare JM, Berger RD. Interaction between neuronal nitric oxide synthase and inhibitory G protein activity in heart rate regulation in conscious mice. *J Clin Invest*. 1998;102:1279–1285.
34. Just A, Faulhaber J, Ehmke H. Autonomic cardiovascular control in conscious mice. *Am J Physiol*. 2000;279:R2214–R2221.
35. McDonald TF, Pelzer S, Trautwein W, Pelzer DJ. Regulation and modulation of calcium channels in cardiac, skeletal, and smooth muscle cells. *Physiol Rev*. 1994;74:365–507.
36. Qu Y, Baroudi G, Yue Y, El Sherif N, Boutjdir M. Localization and modulation of α_{1D} ($Ca_v1.3$) L-type Ca channel by protein kinase A. *Am J Physiol*. 2005;288:H2123–H2130.
37. De Simone A, De Pasquale M, De Matteis C, Canciello M, Manzo M, Sabino L, Alfano F, Di Mauro M, Campana A, De Fabrizio G, Vitale DF, Turco P, Stabile G. Verapamil plus antiarrhythmic drugs reduce atrial fibrillation recurrences after an electrical cardioversion (VEPARAF Study). *Eur Heart J*. 2003;24:1425–1429.
38. Liu J, Dobrzynski H, Yanni J, Boyett MR, Lei M. Organisation of the mouse sinoatrial node: structure and expression of HCN channels. *Cardiovasc Res*. 2007;73:729–738.
39. Azene EM, Xue T, Marban E, Tomaselli GF, Li RA. Non-equilibrium behavior of HCN channels: insights into the role of HCN channels in native and engineered pacemakers. *Cardiovasc Res*. 2005;67:263–273.
40. Mannikko R, Pandey S, Larsson HP, Elinder F. Hysteresis in the voltage dependence of HCN channels: conversion between two modes affects pacemaker properties. *J Gen Physiol*. 2005;125:305–326.
41. Accili EA, Redaelli G, DiFrancesco D. Differential control of the hyperpolarization-activated current (I_f) by cAMP gating and phosphatase inhibition in rabbit sino-atrial node myocytes. *J Physiol*. 1997;500(pt 3):643–651.
42. Chang F, Cohen IS, DiFrancesco D, Rosen MR, Tromba C. Effects of protein kinase inhibitors on canine Purkinje fibre pacemaker depolarization and the pacemaker current I_f. *J Physiol*. 1991;440:367–384.
43. Kaupp UB, Seifert R. Molecular diversity of pacemaker ion channels. *Annu Rev Physiol*. 2001;63:235–257.
44. Bogdanov KY, Maltsev VA, Vinogradova TM, Lyashkov AE, Spurgeon HA, Stern MD, Lakatta EG. Membrane potential fluctuations resulting from submembrane Ca^{2+} releases in rabbit sinoatrial nodal cells impart an exponential phase to the late diastolic depolarization that controls their chronotropic state. *Circ Res*. 2006;99:979–987.
45. Baillie GS, Scott JD, Houslay MD. Compartmentalisation of phosphodiesterases and protein kinase A: opposites attract. *FEBS Lett*. 2005;579:3264–3270.
46. Steinberg SF, Brunton LL. Compartmentation of G protein-coupled signaling pathways in cardiac myocytes. *Annu Rev Pharmacol Toxicol*. 2001;41:751–773.
47. Wong W, Scott JD. AKAP signalling complexes: focal points in space and time. *Nat Rev Mol Cell Biol*. 2004;5:959–970.
48. Jones SA, Boyett MR, Lancaster MK. Declining into failure: the age-dependent loss of the L-type calcium channel within the sinoatrial node. *Circulation*. 2007;115:1183–1190.
49. Naga Prasad SV, Perrino C, Rockman HA. Role of phosphoinositide 3-kinase in cardiac function and heart failure. *Trends Cardiovasc Med*. 2003;13:206–212.